THE PUBLISHING HOUSE
OF THE ROMANIAN ACADEMY

PROCEEDINGS OF THE ROMANIAN ACADEMY, Series A,
Volume 21, Number 3/2020, pp. 273–282

RESEARCH ON THE MITIGATION OF SHAPED CHARGE EFFECT

Adrian MALCIU[1], Constantin-Cristinel PUICĂ[1], Cristina PUPĂZĂ[2], Daniela PINTILIE[1], Florinel IANCU[1]

[1] Military Equipment and Technologies Research Agency, 16 Aeroportului Street, Clinceni, Ilfov, 077025, Romania
[2] "Politehnica" University of Bucharest, Robots and Manufacturing Systems Department,
313 Splaiul Independenţei Avenue, 060042, Romania

Corresponding author: Cristina PUPĂZĂ, E-mail: cristina.pupaza@upb.ro

Abstract. The increase of the ammunition destructive effects has led to the development of various armor types to achieve a high degree of protection for the personnel. The purpose of the paper is to study the impact of a shaped charge hit on a cage armor protection system. Experiments were carried out for a deep understanding of the phenomena occurring at the impact between the shaped charge round and the armor and to include experimental information in the numerical model. The simulation has been performed using an explicit solver. When analyzing the results, the effects of the armor on the threat were explained and aspects regarding possible risks caused by the shock transmitted to the explosive materials were clarified. The novelty of the research consists in the 3D numerical model of the shaped charge grenade performed for an impact phenomenon with the Lee-Tarver equation of state describing the explosive material. The study also explained the source of the explosive initiation.

***Key words**:* simulation, mitigation, shaped charge, round effects, slat armor, Lee-Tarver EOS.

1. INTRODUCTION

Nowadays most armored vehicles offer a relatively high degree of protection against bullets or skulls and fragments resulting from the operation of an artillery shell. The armors on the vehicles have been upgraded so that bullets of infantry munitions or inert projectiles of small caliber cannons no longer cause a threat to the personnel inside the armored box. As a result, besides the development of large caliber cannons, the specialists turned on new types of ammunitions that use the chemical energy contained by energetic materials to penetrate the armor. These materials capable to detonate are also known as high explosives. During the detonation, gases are generated at pressures up to 300 kbar and temperatures about 3000-4000°C [1]. The presence of a confinement envelope in contact with the undetonated explosive charge will interfere with the post-detonation process of the hot gases expansion. The effects on the envelope depend not only on the mechanical properties of the materials but also on the shape and size of the entire explosive charge/envelope system. Besides the omnidirectional radial propulsion of the fragments that typically occurs in the case of explosive projectiles with axial symmetric configuration [2], special arrangements, like planar symmetric [3] or the existence of excavations in the explosive charge [4] may allow the occurrence of directional effects. This phenomenon, named shaped charge effect, appears when a thin liner of ductile material covers an excavation of conical shape collapses in a controlled manner under the action of the detonation wave.

Although in recent years several research papers have investigated the impact mechanism for shaped charges they do not handle much on the mitigation effect obtained by passive armors. Initial simulation studies [5] were reported on the impact of a shape charge jet head with steel rods, but the calculation was performed using a simplified missile and the grenade penetrated the armor in between the bars. Another perspective is the study about the influence of cone angles and liner materials on shaped charge penetrating layered and spaced targets [6]. The research was focused on the diameters of entry, the exit craters and the depth of penetration, only that the material of the target was concrete, usually used for buildings and the velocity of the charge had correspondingly high values.

Beside the shaped charges behavior at impact and the formation of the jet it is necessary to analyze the mechanisms of explosives initiation under different stimuli. In the case of shaped charge impacting slat armor, the explosive initiation by the impact phenomena has to be deeply understood. Therefore, numerical simulations were done with RUSS-2DE hydrocode on a projectile which has a smaller or larger diameter than the failure diameter of the explosive, in this case PBX 9404 [7]. The aim was to observe the formation stages of the detonation. Other studies also investigated the shock-induced detonation of high explosives confined in an open-ended steel cylinder by a normal impact to the cylindrical surface using three-dimensional finite element analysis [8]. Three different shapes of steel projectiles were considered: cube, sphere and square plate. The energetic materials taken into account were the PBXN-110 and LX-17 explosives. The results were focused on the detonation threshold conditions, in terms of velocities. Another interesting work was published by Davison, who determined using 2D and 3D models the detonation threshold conditions for a six-inch shaped charge warhead impacted from the side by 0.50 inches caliber fragment-simulating projectiles at different velocities [9].

The present research deals with modeling and simulation of the impact of a shaped charge grenade on a slat armor taking into account shaped charge effects. The study comprises advanced models of the grenade and corresponding simulation parameters that allowed the explanation of the phenomena observed during experiments. The paper is organized as follows: In the second part a brief overview is performed regarding the shape charge effects, jet formation and the ammunition. The third part analyses the slat armor. Experimental research undertaken with a PG-7 round on a grid target is included in the fourth part of the work. The proposed approach is explained in the fifth part of the work, where novel numerical models supported by simulation addressed the shaped charge effect phenomena. The final chapter summarizes the proposed approach, draws up conclusions and includes future work objectives.

2. SHAPED CHARGE EFFECTS

The shaped charge effect of the explosive charge emerged at the beginning of the 20th century, but its use has spread since the Second World War. At that time Monroe, von Neumann and von Foerster, have discovered that by practicing a cavity on one side of an explosive charge and initiating it from the opposite side will result a deeper penetration than the one caused by an explosive without a cavity. The researchers observed that by placing a metal in the respective cavity with dihedral or conical shape, the effect on the armor increases the perforation depth or the perforation diameter. References to their studies can be found in [10] and [11], because their works are not available in open literature at present. In Fig. 1 a shaped charge and its components are presented.

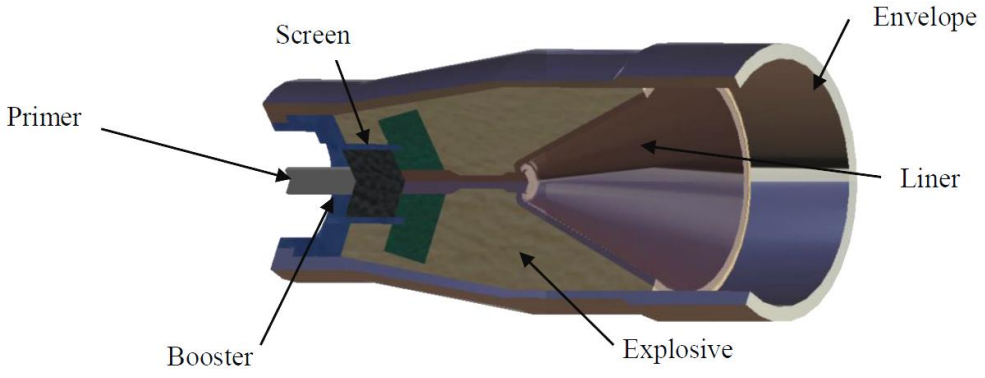

Fig. 1 – The component parts of a shaped charge [10].

2.1. Jet formation

The cumulative effect consists in the concentration of the detonation wave on a certain direction - the axis of the cylindrical or conical cavity. This is done by the refraction of the shock wave in the cavity and its exit from a medium with a propagation velocity of thousand meters per second in the air.

Devoted literature [3, 11] describes the phenomenon of the shaped charge jet formation according to the stages illustrated in Fig. 2. All the elements on the circular crown are projected on the symmetry axis where they are divided into:

– the slug that contains the bulk of the liner mass and moves at low speeds (500–1000 m/s);

– a relatively small but very fast mass jet (11000–12000 m/s), where most of the kinetic energy of the liner is found.

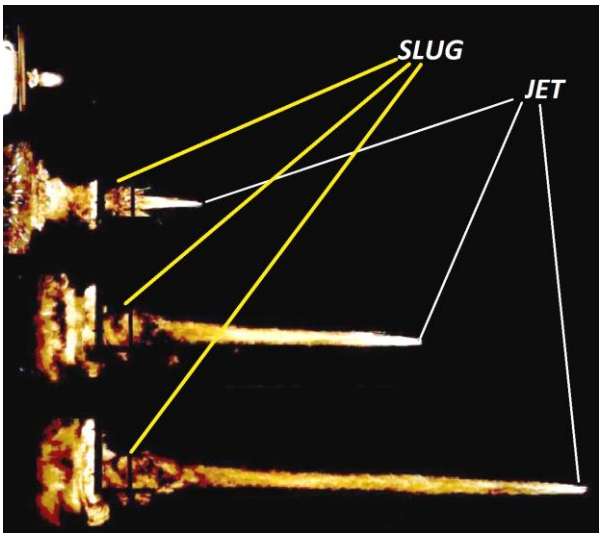

Fig. 2 – Jet formation stages.

Shaped charges are the explosive charges provided with a cavity in which a metallic liner is introduced which, as a result of the detonation of the explosive, forms a jet capable of punching or cutting metallic materials [3]. For military purposes, they are used to penetrate the armor of a combat machine, thereby creating a hole through which the gaseous products resulting from the detonation of the explosive penetrate into the armored case causing injuries or even death of the staff, due to high temperatures and high pressures. The perforating power of these rounds can destroy military objectives such as buildings, control points, but can also affect important components of the military vehicles (motor, wheels, tracks, etc.), immobilizing them, too.

In order to maximize the effect of the shaped charge, the following conditions must be met simultaneously to ensure the shaped charges operation:

– symmetry of the cavity and of the metallic lining;

– initiation of the explosive charge must occur from the opposite side of the cavity, from a point that is mandatory on the axis of symmetry;

– the homogeneity of the explosive material, but also of the material from which the cumulative funnel is made;

– the thickness of the liner metal must be constant along the cone generator.

2.2. RPG-7 Ammunition

PG-7 is a product whose operation is based on the use of the cumulative effect. It is an antitank ammunition, fired by the RPG-7 reactive grenade launcher. The system was developed in the Soviet Union and used by the Russian army in 1961. Nowadays, two variants of the PG-7, PG-7V and PG-7VM are produced in Romania. The main features of the round that were taken into account in the numerical model are included in Table 1 [3].

The most important characteristic from Table 1 is the penetration depth the jet can reach in a RHA (rolled homogeneous armor) steel. A tank or a carrier cannot have an armor thickness that totally prevents the penetration caused by the cumulative jet of a PG-7 grenade. That is why manufacturing of composite armors or protective systems were required.

Table 1

PG-7VM round features [3]

Features		Value/type
caliber of grenade	launcher caliber	40 mm
	grenade caliber	70.5 mm
length	round	959 mm
grenade velocity	initial	140 m/s
	maximum	350 m/s
shooting	rate	4–6 rounds/min
	distance maximum from support	500 m
	distance for a direct round when the height of the objective is 2 m	330 m
mass	round	2.2 kg
	grenade	1.8 kg
penetration capacity in armor plate		300 mm
explosive		A IX-1
propellants	PRTF-200 propelling	220 g
	NBL 42 launching	124 g

3. SLAT ARMOR

Armored layouts can be classified into three groups, depending on their action: active, reactive and passive armors [12, 13].

The slat armor is a passive protection system and contains metal bars or nets of steel or textile wires that act against cumulative rounds on the strength of the following phenomena: the deformation of the shaped charge case and explosive cracks that block the normal operating conditions of the round. In the case of PG-7 grenade (Fig. 3), the initiation of the explosive charge is carried out by means of the electric impulse transmitted through the head fuse towards its bottom to the electric detonator, a phenomenon that takes place via two circuits [14]. The first circuit is an external one: ballistic coat – metal grenade shell – electric detonator and the other is an internal one, conductor cone – liner – detonator. Thus, due to the impact with the net or the protective grid, the deformation of the coat is achieved until the contact with the conductive cone occurs, causing the electric signal to be short-circuited.

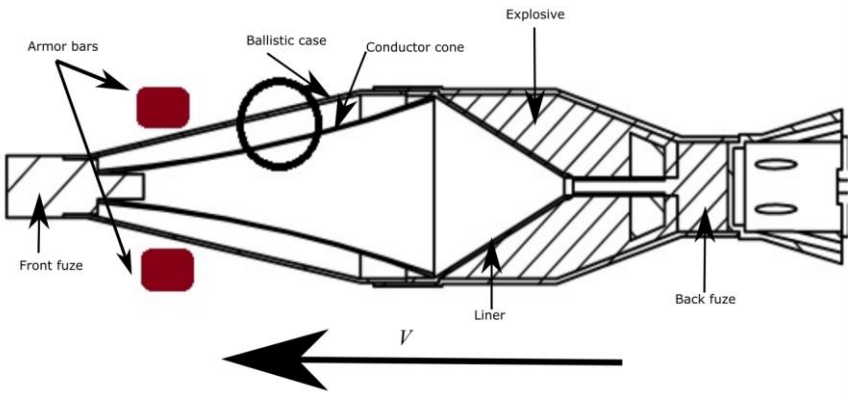

Fig. 3 – The slat armor protection mechanism [14].

The main disadvantages of this type of armor are:

– the fairly large probability of striking the bars/yarns of the grilles/armor nettings, in respect to the remaining free surface. Taking into account that the fuse will work at any point the impact occurs, the operation of the cumulative charge is not jeopardized in any way;

– the destruction on a relatively large surface during the event of a goal, but especially if the round works. This is the reason why the military vehicle will have great vulnerability to the upcoming hits.

Considering these drawbacks, it is worth stating that the slat armor has advantages that have to be taken into account when choosing a protection system against PG-7: reduced manufacturing costs, large number of

materials that can be used, low density on the surface unit compared to other passive armor types, easy installation – allowing quick replacement of the component panels on the battlefield without the need of special tools.

4. EXPERIMENTAL RESEARCH

The cage passive armor is used for most military vehicles due the benefits outlined above. As a consequence, it is very important to experimentally investigate the impact of the shaped charges on the armored arm and to evaluate the mitigation effect.

For a deep understanding of the phenomena occurring at the time of impact and to include experimental information in the simulation model, the PG-7 cumulative rounds were fired on a bar grid target placed at a distance d of 45 cm from the witness plate (Figs. 4 to 7). This witness plate was included as a basic armor of a fighting vehicle and highlights the way the grenade round operates.

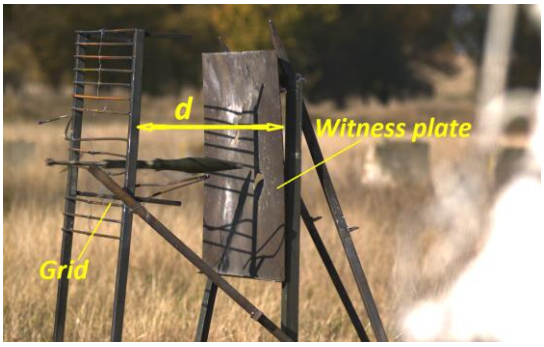

Fig. 4 – The round do not hit the bar.

Fig. 5 – The beginning of the jet formation at t = 2.1 ms after the round passed between the bars

Fig. 6 – PG-7 round hits a bar.

Fig. 7 – The explosive transformation observed at t = 2.6 ms after the impact between the round and the witness plate.

The tests emphasized two cases, captured by ultra-fast camera. In the first one (Figs. 4 and 5) the round has entered through the two bars of the grid without any contact and after t = 1.7 ms it operated properly (Fig. 5). In the second case (Figs. 6 and 7), the round was deformed by the upper bar (Fig. 6). After t = 2.1 ms, the plate was hit by grenade and the fuze did not initiate the explosive charge. Then, the grenade was flattened up to the rocket engine nozzle due to the inertial force. It was important to notice that, although the electrical impulse was not transmitted to the detonator, at time t = 2.6 ms after the first contact between the round and the witness plate, an explosive transformation was observed from the images captured by the ultra-fast camera (Fig. 7).

The conclusion was that the initiation can have the origin in the back fuze and if this takes place earlier than the one observed in Fig. 7 it is possible that a jet formation may occur. Experiments revealed that it was necessary to study this phenomenon using an explicit dynamic solver, because the detonation can be initiated by the PETN (Pentaerythritol tetranitrate) charge from the booster and this phenomenon is hard to be observed from the images captured by ultra-fast camera.

5. SIMULATION OF THE IMPACT OF A SHAPED CHARGE HIT ON A CAGE ARMOR

5.1. Model preparation

The simulation of the impact phenomenon with all the details involved (i.e. the full stroke and the whole bar grid) is very time-consuming and requires parallel computing. Therefore a simplified model that works in accordance with real shooting conditions picked out during the experiments was developed. The shot was represented by the cumulative grenade, and the grille was taken into account by a single bar with 10 mm diameter, embedded at both ends and disposed at a distance d of 45 cm from the armor plate. This distance was exactly the same with the one considered during experiments.

Mesh generation is always an important issue in an explicit dynamic simulation and assures accurate results when a fine and regular mesh is obtained. Since all the components of the assembly have a complex geometry, a devoted pre-processing system has been used in order to create the computational model. The mesh strategy for the grenade was the most important step because the whole study is focused on this component. That is why first a 2D model has been performed in a CAD system and then the geometry was imported into the project, where the 3D model has been generated (Fig. 8). To ensure the best numerical results a structured fine mesh has been generated using 184 blocks, as presented in Fig. 8. The virtual model counts 1,941,768 finite elements (Fig. 9). After mesh optimization, the entire model was imported in ANSYS AUTODYN (Fig. 9), the explicit solver devoted to shock and detonation issues. The simulation was performed on a dual server with 8 cores each CPU and 128GB RAM. The computation time was between 90 and 150 hours for each run.

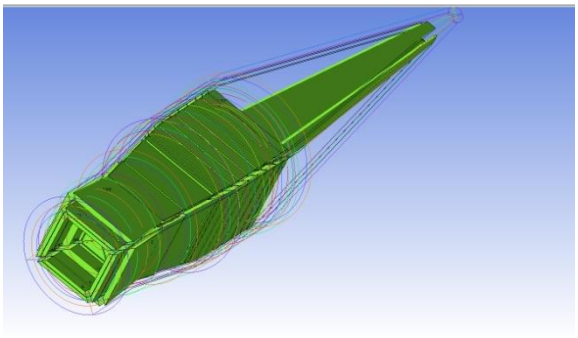

Fig. 8 – Geometry edges and the blocks attached to geometry.

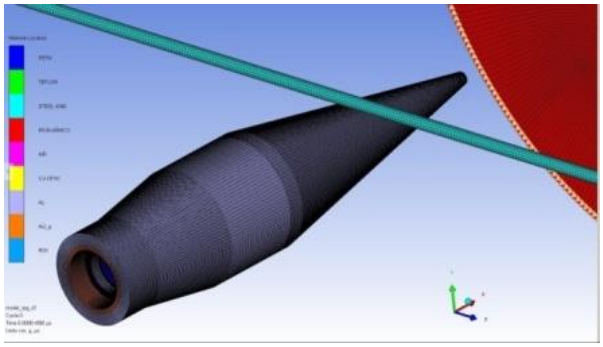

Fig. 9 – The computational model and grenade fine mesh

The position of the bar at the time it interacts with the grenade was also taken into account in the simulation model. Because it is almost impossible to establish the relative position of the bar at the impact moment only from the images captured by the ultra-fast camera and in order to cover the impact area from the experimental conditions, the simulation model was computed for three cases, as it is illustrated in Figs. 10, 11 and 12. Thus, the simulation started from the middle of the round up to a position that has an influence in the deformation of the grenade metallic envelope, in correspondence to the cage armor principle presented in section 3. For each case the bar has been placed almost in contact with the ballistic cone of the grenade, the maximum distance between them being of 1 mm (Figs. 10, 11 and 12).

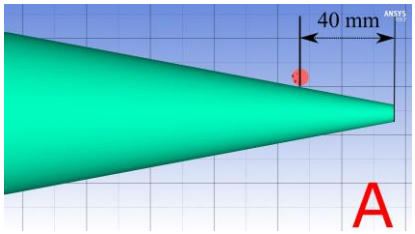

Fig. 10 – Simulation case A.

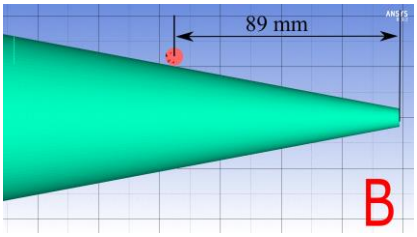

Fig. 11 – Simulation case B.

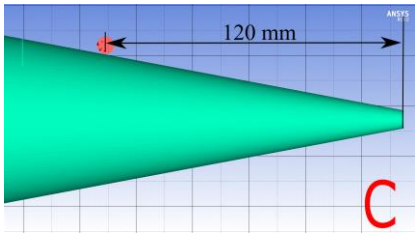

Fig. 12 – Simulation case C.

The materials for all grenade components, bar and board were defined as follows: the grenade case was of Aluminum alloy T4 and the lens of Teflon and electrolytic copper CU-OFHC. Energetic materials were chosen from the AUTODYN library or were defined as follows: for A IX-1 – an equivalent explosive with

the same sensitivity properties, named RDX, considering that A IX-1 contains 94-95% RDX in its composition, and pentrite (PETN) for the back fuse detonator (Fig. 3). Because a potential impact initiation of the explosives was required, PETN and RDX (cyclotrimethylenetrinitramine – a more energetic explosive than TNT) had to be defined by an equation of state specific to this phenomenon. Thus, the explosives behavior is described by the Lee-Tarver equation of state (EOS) (1) in the solver algorithm, which has the following form [15, 16]:

$$\frac{\mathrm{d}F}{\mathrm{d}t} = I(1-F)^b(\mu - a)^x + G_1(1-F)^c F^d P^y + G_2(1-F)^e F^g P^y \,, \tag{1}$$

where F represents the initiated fraction of the explosive, μ - the compressibility of the explosive, P is the pressure, and I, b, a, x, G_1, c, d, y, G_2, e, g and z are unknown constant parameters. The equation comprises three terms. The first one describes how the explosive initiates according to its compressibility, the second one describes the formation of the hot spots until they coalesce, and the third term, the growth of the reaction zone and the expansion of the detonation products after the hot spots coalesce.

The properties, the equation of state and the coefficients of energetic material are presented in Table 2. The solver material library does not provide all the material models described by Lee-Tarver equation of state (1). For JWL (Jones-Wilkins-Lee) equation of state parameters for A IX-1, the values presented in Table 2 were introduced from the reference [18]. A, B, R_1, R_2 and ω are constants and their values, for many common explosives, are determined from dynamic experiments.

Table 2

A IX-1 Lee Tarver parameters

Reactants JWL EOS	A = 8.524 Mbar	B = 0.1802 Mbar	R_1 = 4.6	R_2 = 1.3	ω = 0.38	ρ = 1.66 g/cm^3
Products JWL EOS	A = 9522 Mbar	B = –0.05944 Mbar	R_1 = 14.1	R_2 = 1.41	ω = 0.8867	
Reaction Rates	I = 20000 μs^{-1}	a = 0.09 x = 20	G_1 = 3.1 λ_{G1max}= 0.5	c = 0.667 d = 0.111 y = 1	G_2 = 400 λ_{G2min} = 0	e = 0.333 g = 1 z = 2

As mentioned before, the main compound of A IX-1 explosive is RDX. As such, because of the lack of information about the RDX EOS parameters, a sequence of simulation experiments have previously been done in AUTODYN to tune the behavior of A IX-1 with the experimental findings. The only reference about a suitable choice of the Lee-Tarver EOS parameters [17] specifies that if the explosive is not characterized by the Lee-Tarver model, another explosive component may be used, but the a parameter has to be adjusted accordingly, in order to match the experiment. If no experiment is available, a parameter has to be estimated using the equation:

$$a = 1 - \rho/\rho_{TMD}\,, \tag{1}$$

where ρ is the material density and ρ_{TMD} is a theoretical maximum solid density.

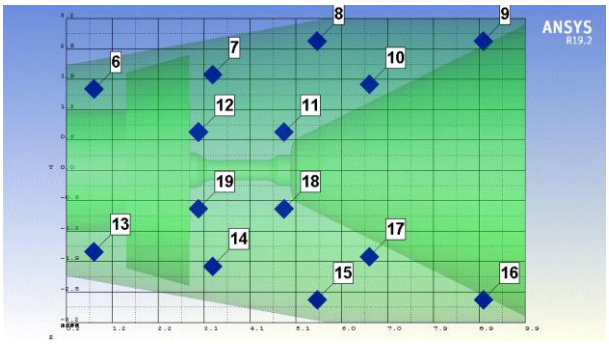

Fig. 13 – Gauge positions in X-Y plane.

The A IX-1 explosive density used in the literature is $\rho = 1.66$ g/cm^3 [18] and the theoretical maximum density of RDX is $\rho_{TDM} = 1.82$ g/cm^3 [19]. Under these conditions, if we solve eq. (2) the *a* parameter value is $a \cong 0.09$. An initial velocity of $v = 280$ m/s was set, taking into account that this parameter can reach a maximum value of 300 m/s during the rocket engine active time. The virtual fixture of the bar and the fixed boundary of the armored plate have also been considered.

For monitoring the state parameters and for a good control of the results quality, several virtual sensors (gauges) were placed at specific locations in the *XY* plane of the explosive material, in the proximity to the liner and also close to the grenade external case (Fig. 13). This allowed the observation of the explosive behavior under the compressive waves generated during the impact with the bar.

5.2. Simulation results

Simulation was an important approach since it allowed the observation of the energetic materials physical characteristics from the warhead during the impact between the grenade and the steel bar for three different cases. Another important goal was to monitor the plot contours of the burned fraction from the explosive cell, which in AUTODYN represents the *ALPHA* coefficient, namely the burned fraction *F* from the Lee-Tarver EOS (1). Therefore, after it was observed the way the bar deforms the grenade, the simulation cases were stopped as follows: A at $t = 810$ μs, after the bar has been broken; B at $t = 612$ μs, because of the same reason as for the first case; C – at $t = 480$ μs, when the bar has been deformed since the contact with the grenade components did not exist. Figures 14, 15 and 16 illustrate the *ALPHA* plot contours of the explosive material (for *ALPHA* between 0 and 1) for each simulated case. From these figures it can be stated that the explosive did not detonate, the elements with *ALPHA*=1 or nearly 1 being only few cells (the red ones) spread into the affected energetic material. This fact proves that there is no probability of reaching the critical volume for initiation the growth of the reaction zone through the coalesce of the hot spots.

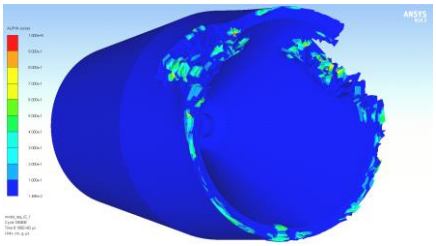

Fig. 14 – *ALPHA* plot for case A: t =810 μs.

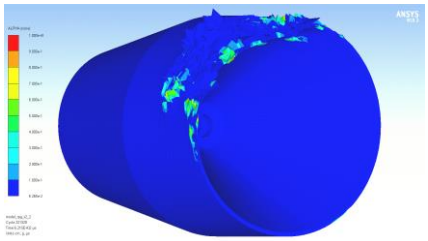

Fig. 15 – *ALPHA* plot for case B: t =612 μs.

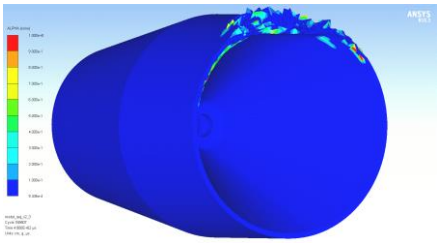

Fig. 16 – *ALPHA* plot for case C: t =480 μs.

In order to have a clear picture of the shock influence into the entire explosive domain, time history plots of the *ALPHA* coefficient (Figs. 17, 18 and 19) were saved for Gauges 7, 8, 10, 11 and 12.

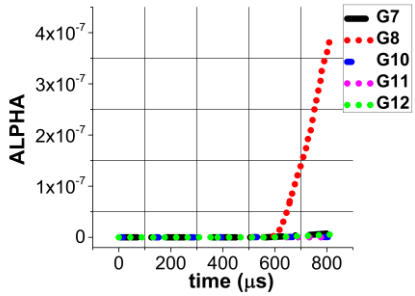

Fig. 17 – *ALPHA* plot for case A.

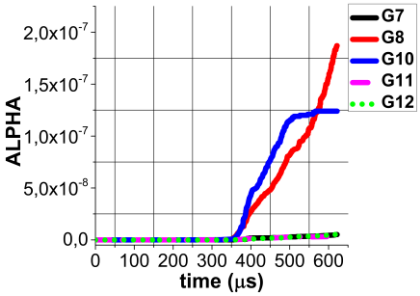

Fig. 18 – *ALPHA* plot for case B.

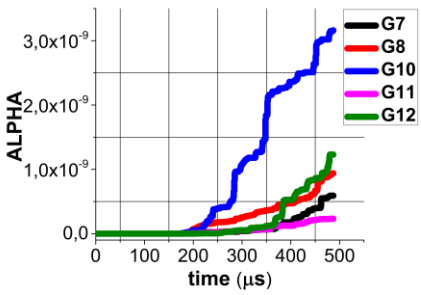

Fig. 19 – *ALPHA* plot for case C.

Analyzing the three plots from Figs. 17, 18 and 19 it can be concluded that the probability of the energetic material initiation inside the grenade following the impact with the bar is very low.

In order to initiate the detonation the coefficient of the burnt explosive fraction has to reach a value of 1 or nearly 1 and the elements have to coalesce in the hotspots after a growth in volume until the detonation

is initiated. In these three cases, the maximum values of *ALPHA* coefficient were low: for case A *ALPHA* was $4 \cdot 10^{-7}$; for case B – *ALPHA* $\approx 2 \cdot 10^{-7}$ and for case C – *ALPHA* $\approx 3.1 \cdot 10^{-9}$. This means that the detonation did not auto propagate. The impact-induced shock also generated a relatively low pressure with a maximum value of $P \approx 0.25$ kbar, recorded by Gauge 10 for case A. This value is small compared to the pressure reached when the detonation takes place, that is $P = 273.5$ kbar [18].

In conclusion, the material model was truthfully validated, the simulation results being similar to the behaviour of the explosive from the warhead of PG-7 round, whose detonation has not been initiated at the interaction with the bar, as happened during the experiments (Chapter 4), but the calculation took tens of hours for each case. Once the impact between the round and the bar has been clarified, the study of the grenade-armor plate interaction was continued with a 2D axisymmetric model. With this approach, the computation time was reduced to only 50 hours. In this new model the ballistic front cone was not considered and the grenade was subjected to an impact perpendicular on a virtual fixed wall, that cannot be deformed (Fig. 20). Initial conditions and material patterns remained similar to those of the 3D model. The velocity of the grenade was $v = 280$ m/s, the dimensions and material properties were the same. The essential modification was the use of advanced capabilities of the solver through which all the materials have been loaded in a Euler-Godunov calculus domain.

The parameter tracked during this new simulation was also the *ALPHA* parameter (Fig. 21), until a critical volume was observed. In the Lee-Tarver EOS (1) the critical volume is considered the minimum volume of the material where the *ALPHA* coefficients of the elements reach the value of 1 and, starting from this point, the detonation will be transmitted in the entire explosive.

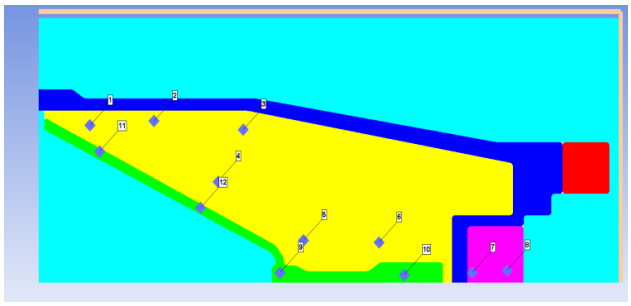

Fig. 20 – Axisymmetric model.

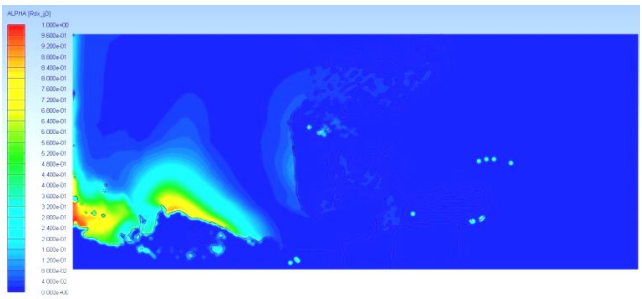

Fig. 21 – *ALPHA* coefficient at time $t = 264$ μs.

Figure 21 illustrates that at time $t = 264$ μs the *ALPHA* coefficient near the liner funnel peak area has reached the value of 1 and the red zone that represents the hot spots generated by the shock impact can be clearly observed. Hence, the detonation can self-propel in the entire explosive material.

6. CONCLUSION

The research provided explanations regarding the source and the explosive transformation that occur during the impact between a grenade and a steel plate using explicit dymamic simulation models. The study proved that the explosive transformation detected during the experiments was determined by the detonation of the explosive, due to the reach of a threshold value of the impact energy that initiates the detonation.

Three simulation cases on a 3D model aimed to investigate the possibility that the explosive material can be initiated by impacting the bar. The model has been validated, showing a good match with the experimental outcomes, during real shooting tests. On the other hand, the simulation using an axisymetric model dramatically reduced the computation time and proved that the hypothesis of the detonation initiation from the back fuze booster is not valid, because the values of *ALPHA* parameter are not appropriate for this scenario. The novelty of the approach consists in the simulation procedure in which the 3D model for the explosive material moving to the target was described by the Lee-Tarver EOS.

Cage armours are important for military vehicles, but do not provide a high level of protection against shaped charge rounds, because of the probability that the grenade fuze can hit a bar of the armour. From that moment, the explosive is instantaneously initiated and the shaped charge will form the jet that will penetrate

the base armour. There is also the situation presented in this work, when the explosive transformation still takes place, although the armour works properly. This drawback requires even a deeper study. Further work will be focused on the definition of a RDX based explosive in the material library of explicit solvers that can highlight the role of every Lee-Tarver parameter.

ACKNOWLEDGEMENTS

This work has been supported by Military Equipment and Technologies Research Agency (Clinceni, Romania), being a subject of a project included in the Research and Development Sectoral Plan of Ministry of National Defence, Romania.

REFERENCES

1. A.N. ROTARIU, C. DIMA, E. TRANA, C. ENACHE, F. TÎMPLARU, L.C. MATACHE, *Uninstrumented measurement method for granular porous media blast mitigation assessment*, Experimental Techniques, **40**, *3*, pp. 993-1003, 2016.
2. E. TRANĂ, A. ROTARIU, F. BUCUR, *Numerical simulation study on the ring fragmentation*, Military Technical Academy Review, **XXV**, *2*, pp. 179-188, 2015.
3. C. ENACHE, E. TRANĂ, T. ROTARIU, A. ROTARIU, V.T. ŢIGĂNESCU, T. ZECHERU, *Numerical simulation and experimental tests on explosively-induced water jet phenomena*, Propellants, Explosives, Pyrotechnics, **41**, *6*, pp. 1020-1028, 2016.
4. A.N. ROTARIU, *Balistică terminală. Formarea și accelerarea impactorilor*, Editura Academiei Tehnice Militare, Bucharest, 2017.
5. K. SYBILSKI, R. PANOWICZ, D. KOŁODZIEJCZYK, D.T. NIEZGODA, *Validation studies of the simplified model of the missile with cumulative head*, Journal of KONES Powertrain and Transport, **19**, *3*, pp. 415-420, 2012.
6. W. CHENG, Xu WENLONG, S. CHUNG, K. YUEN, *Penetration of shaped charge into layered and spaced concrete targets*, International Journal of Impact Engineering, **112**, pp. 193-206, 2018.
7. V.Y. KLIMENKO, *Two mechanisms of explosives initiation by the impact of a cylindrical projectile*, AIP Conference Proceedings, **429**, pp. 381-382, 1998.
8. J. CHEN, H.-K. CHING, F. ALLAHDADI, *Shock-induced detonation of high explosives by high velocity impact*, Journal of Mechanics of Materials and Structures, **2**, *9*, pp. 1701-1721, 2007.
9. D. DAVISON, *Three-dimensional analysis of the explosive initiation threshold for side impact on a shaped charge warhead*, Insensitive Munitions and Energetics Technology Symposium, 1997.
10. C. ENACHE, *Încărcături cumulative. Soluții constructive. Aplicații*, Academia Tehnică Militară, Bucharest, 2016.
11. D. CARLUCCI, S. JACOBSON, *Ballistics: theory and design of guns and ammunition*, CRC Press, 2018.
12. P.J. HAZELL, *Armor: materials, theory, and design*, CRC Press, Taylor & Francis Group, 2015.
13. D. TANSEL, *Ballistic penetration of hardened steel plates*, MSc Thesis, Middle East Technical University, Mechanical Engineering Department, Ankara, 2010.
14. C.H.K. YAP, *The impact of armor on the design, utilization an survivability of ground vehicles: the history of armor development and use*, MSc Thesis in Mechanical Engineering, Naval Postgraduate School, Monterey, California, 2012.
15. E.L. LEE, C.M. TARVER, *Phenomenological model of shock initiation in heterogeneous explosives*, American Institute of Physics, Livermore, 1980.
16. H.J. VERBEEK, *Shock initiation modeling of explosives*, TNO report PML 1997-A33, Rijswijk, 1997.
17. G.W.J. MCINTOSH, *Explosive modeling using LS-DYNA – A user's guide*, Defense R&D Canada-Valcartier, Technical Memorandum, February 2014.
18. J. SELESOVSKY, J. PACHMAN, M. KÜNZEL, *Numerical simulation of explosively driven aluminum flyer acceleration*, New trends in Research of Energetic Materials, Pardubice, 2016.
19. D.M. HOFFMAN, *Density distributions of cyclotrimethylenetrinitramines (RDX)*, U.S. Department of Energy, Lawrence Livermore National Laboratory, 2002.

Received July 29, 2019